Mater. Res. Soc. Symp. Proc. Vol. 925 © 2006 Materials Research Society 0925-BB02-07

# Calcium Phosphate Bioceramics with Tailored Crystallographic Texture for Controlling Cell Adhesion

Hyunbin Kim[1], Renato P. Camata[2], Sukbin Lee[3], Gregory S. Rohrer[3], Anthony D. Rollett[3], Kristin M. Hennessy[4], Susan L. Bellis[4], and Yogesh K. Vohra[2]

[1]Department of Materials Science and Engineering, University of Alabama at Birmingham, Birmingham, AL, 35294

[2]Department of Physics, University of Alabama at Birmingham, Birmingham, AL, 35294

[3]Department of Materials Science and Engineering, Carnegie Mellon University, Pittsburgh, PA, 15213

[4]Department of Physiology and Biophysics, University of Alabama at Birmingham, Birmingham, AL, 35294

## ABSTRACT

The orientation distribution of crystalline grains in calcium phosphate coatings produced by pulsed laser deposition was investigated using an X-ray pole-figure diffractometer. Increased laser energy density of a KrF excimer laser in the 4–7 J/cm$^2$ range leads to the formation of hydroxyapatite grains with the *c*-axis preferentially aligned perpendicularly to the substrates. This preferred orientation is most pronounced when the plume direction of incidence is normal to the substrate. This crystallographic texture of hydroxyapatite grains in the coatings is associated with the highly directional and energetic nature of the ablation plume. Anisotropic stresses, transport of hydroxyl groups, and dehydroxylation effects during deposition all seem to play important roles in texture development. Studies of mesenchymal stem cell/biomaterial interactions show that the surfaces with an oriented distribution of hydroxyapatite grains promote significantly better cell adhesion than surfaces with random grain distribution.

## INTRODUCTION

The excellent biocompatibility and bioactivity of calcium phosphate nanostructured surfaces offer a promising pathway for controlling key bioengineering processes such as cell cycle regulation, gene transfer, and patterned cell growth. The ionic dissolution products from these materials are known to affect, for example, the cell cycle of cells responsible for bone tissue formation. This effect may be genetically mediated as expression of various families of genes has been shown to be upregulated by $Ca^{2+}$ ions. These include genes for cell-signaling molecules, growth factors, DNA synthesis and repair, and extracellular matrix proteins. Among the many nanoscale physical characteristics of calcium phosphates that may influence cell activity, its crystallographic texture is one of the least investigated. Yet, crystallographic texture is one of the essential microstructural features that determine the properties of polycrystals. Textures have been extensively studied in metals, geological materials, and selected ceramics. Preferred orientations in biologically relevant ceramics have received little attention. Naturally occurring bioceramics such as calcium phosphates often exhibit preferred orientations resulting from highly specific biological processes. These textures

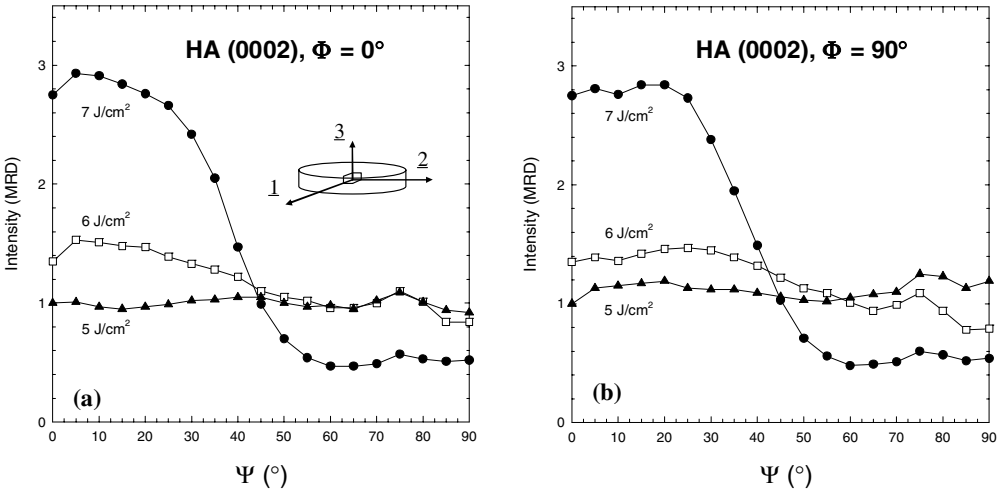


**Figure 1.** The sectional profile of X-ray pole figures for the HA (0002) reflections from coatings deposited at 600 mTorr at 650 °C with different laser energy densities of 5 J/cm$^2$, 6 J/cm$^2$, and 7 J/cm$^2$ for the cut (a) at the planes containing the sample direction 1 and 3 (Φ= 0°) (b) at the planes containing the sample direction 2 and 3 (Φ= 90°).

affect the biological and biomechanical performance of hard tissues such as bone and tooth [1]. Texturing has also been observed in synthetic calcium phosphates that are coated onto metallic implants in dentistry and orthopedics to improve implant integration with adjacent bone tissue [2-6]. Recent studies have shown that the crystallographic texture of calcium phosphate-coated implants may significantly affect osseointegration [7,8]. This suggests that calcium phosphates with surfaces exhibiting tailored crystallographic texture may enable a new level of control of processes such as cell adhesion, differentiation, and proliferation. In this study, we report how pulsed laser deposition (PLD) can be used to produce calcium phosphate coatings with controlled crystallographic texture that may be relevant in controlling cell activity.

## EXPERIMENTAL DETAILS

Calcium phosphate coatings of thickness 1–3 m were deposited by PLD ($9\times10^{-7}$ Torr base pressure) at substrate temperatures of 650–730 °C and Ar/$H_2O$ atmosphere of 400–800 mTorr using a KrF excimer laser (248 nm, 5–7 J/cm$^2$, 30 Hz) [9]. Ablation targets were prepared by compressing a hydroxyapatite powder [$Ca_{10}(PO_4)_6(OH)_2$] (HA) (97.5 % purity). Coatings were deposited on flat, polished, and clean Ti-6Al-4V substrates and the orientation of crystalline grains was studied by X-ray diffraction (XRD) with Cu K radiation (1.5418 Å) in reflection geometry with a standard four-circle goniometer. X-ray pole figures were collected for the HA (0002) and (22$\bar{4}$2) reflections by varying the polar angle, Ψranging from 0° to 85°and the azimuthal angle, Φ ranging from 0° to 360° with a step increment of 5° and a scan time of 4 s per step. The pole figures were corrected for background empirically measured for each sample and

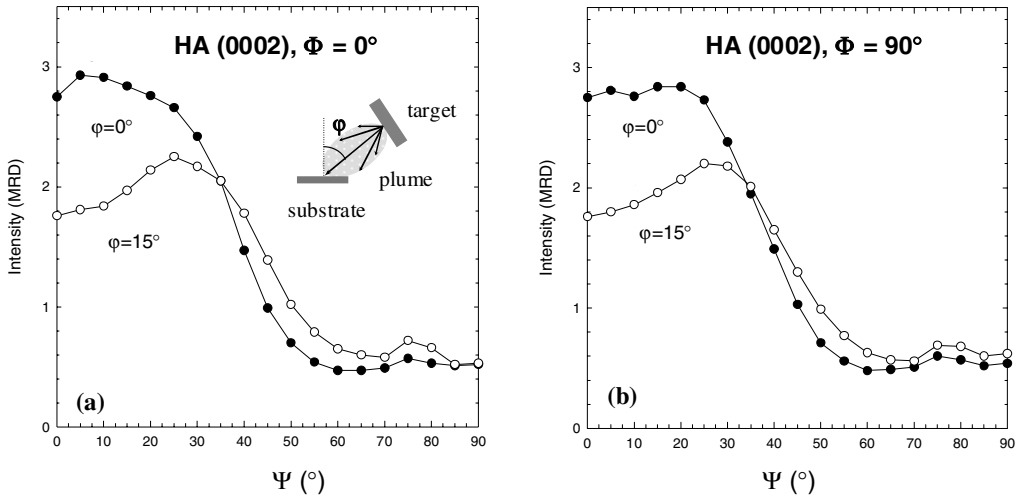


**Figure 2.** The sectional profile of X-ray pole figures for the HA (0002) reflections from coatings deposited at 600 mTorr at 650 ℃ with a laser energy density of 7 J/cm$^2$ at different incident angles of ablated plume for the cut (a) at the planes containing the sample direction 1 and 3 (Φ= 0°) (b) at the planes containing the sample direction 2 and 3 (Φ= 90°).

defocusing of the incident beam adjusted using a randomly oriented HA coating. The recalculated pole figures from orientation distribution (OD) constructed using WIMV algorithm in popLA package [10] had the error less than 1 % when compared with the measured pole figures. Cell adhesion and morphology of human mesenchymal stem cells (MSCs) on the HA coatings was examined as described elsewhere [11]. MSCs were seeded onto the HA coatings and allowed to adhere for 1 h at 37 °C. After several washes with phosphate buffered saline (PBS) to remove nonattached cells, adherent cells were fixed with 3.7 % formaldehyde/Tris-buffered saline (TBS) and permeabilized in TBS containing 0.2 % Triton X-100. The cellular actin cytoskeleton was labeled with phalloidin conjugated to a green fluorescent dye (Alexa 488, Molecular Probes), and cells were subsequently visualized by fluorescent microscopy. To quantify cell attachment, adherent cells were counted from 3 distinct micrographic fields.

## DISCUSSION

X-ray pole figures of HA coatings produced in various deposition conditions were used to study the effect of laser energy, plume direction of incidence, and background pressure on the crystallographic texture of polycrystalline HA coatings whose reflections are well indexed to the HA hexagonal lattice ($a$ = 9.424 Å, $c$ = 6.879 Å, $P6_3/m$) in XRD scans. Figure 1(a) and (b) show the sectional profile of X-ray pole figures of HA coatings deposited with different laser energy densities. As the laser energy density increases, the HA (0002) pole density in the coatings increases in the direction perpendicular to the coatings (Ψ= 0°). The pole figures for the coating deposited at 5 J/cm$^2$ show random distribution of HA (0002) poles with respect to the sample directions 1, 2, and 3 (defined in the inset of Figure 1(a)). In the pole figures for the coating

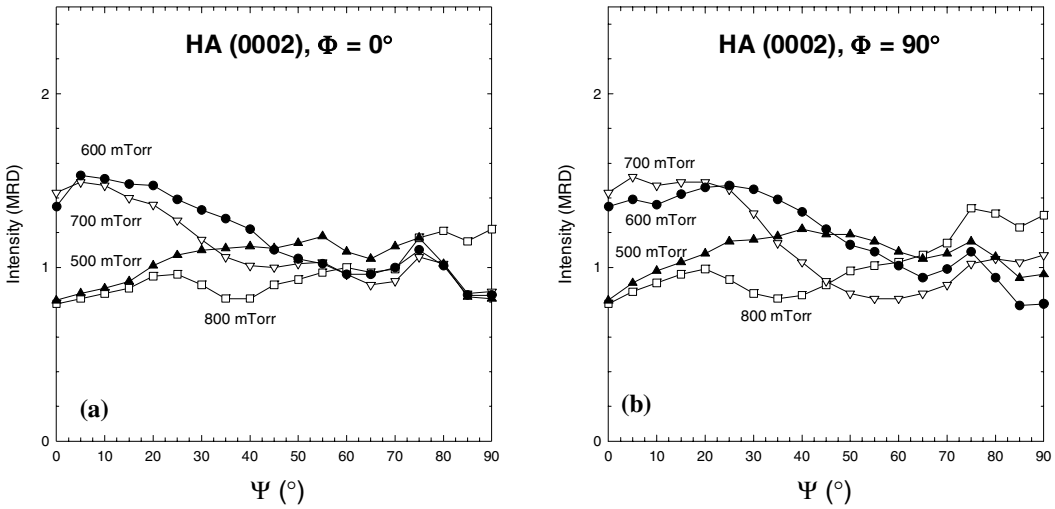


**Figure 3.** The sectional profile of X-ray pole figures for the HA (0002) reflections from coatings deposited at 650 ℃ with a laser energy density of 6 J/cm$^2$ at normal incidence of the plume at different Ar/$H_2O$ pressures for the cut (a) at the planes containing the sample direction 1 and 3 (Φ= 0°) (b) at the planes containing the sample direction 2 and 3 (Φ= 90°).

deposited at 6 J/cm$^2$, the HA (0002) poles appear around the sample direction 3 which indicates the direction perpendicular to the film surface. For the coating deposited at 7 J/cm$^2$, the HA (0002) poles are strongly aligned along the direction perpendicular to the coating. As seen in Figure 1(a) and (b), there is cylindrical orientation symmetry about the surface normal of the coatings, which indicates a fiber texture. This texture is probably caused by the high compressive stress along the normal to the substrate during PLD and the anisotropic elastic modulus of the HA crystals. High-velocity depositing species during PLD leads to a strong stress along the substrate normal. The lower compressibility of HA along its *c*-axis favors the crystallization of the HA grains with the *c*-axis parallel to the direction of maximum stress in order to minimize strain energy [12].

Coatings were also deposited for different values of the angle φ between the symmetry axis of the plume and the direction normal to the substrate as illustrated in the inset of Figure 2(a). The sectional profile of X-ray pole figures shown in Figure 2(a) and (b) reveals a change in the orientation of HA grains in the coatings as a function of the angle of incidence φ The density of the HA (0002) poles in the coating deposited at φ= 0° significantly increases near the substrate normal (Ψ= 0°) and the maximum intensity is higher than the one in the coating deposited at φ= 15°. As the density of HA (0002) poles along sample direction 3 decreases (φ = 15°), the poles spread out slightly while preserving an axial symmetry about the direction 3. For φ> 15° the HA (0002) reflections overlap with the (130) reflections of tetracalcium phosphate (TTCP). The generation of HA orientation distributions in this case requires careful deconvolution of the two peaks involved, which we have not attempted in this study, and therefore pole figures for φ> 15° are not included. Hence, HA texture development is related to the plume

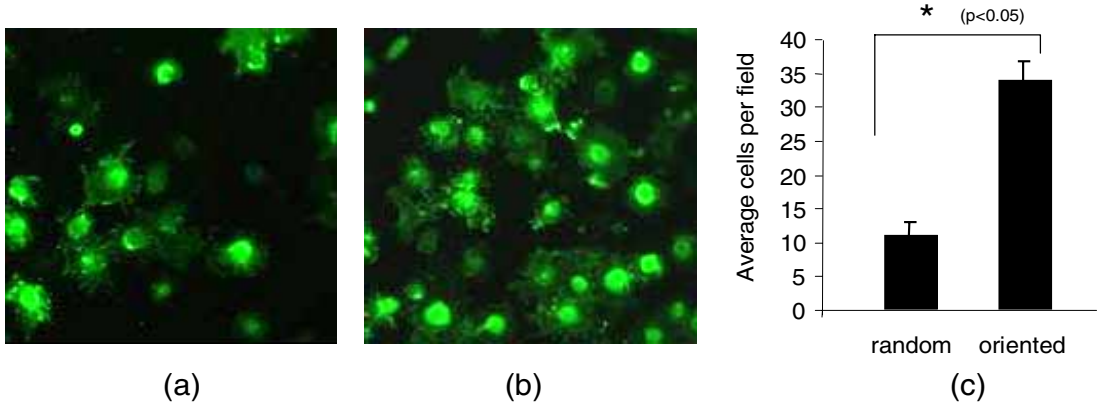


**Figure 4.** Fluorescent microscopic images of cells adherent to randomly oriented hydroxyapatite coatings (a) and *c*-axis textured hydroxyapatite coatings (b). Quantification of adherent cells from 3 distinct microscopic fields reveals that cells adhere in significantly greater numbers to the textured HA coatings (c).

directionality. Less texture at high values of φmay also be related to the formation of inclusions of tetracalcium phosphate [$Ca_4(PO_4)_2O$] (TTCP), which is a dehydrated calcium phosphate compound with the monoclinic structure ($a$ = 7.018 Å, $b$ = 11.980 Å, $c$ = 9.469 Å, $\alpha = \gamma = 90°$, $\beta = 90.88°$, $P2_1$). Higher values of φapparently lead to less incorporation of hydroxyl groups (OH) resulting in more TTCP formation and randomly oriented HA.

Figure 3(a) and (b) show the sectional pole figures of HA in the coatings obtained at different background pressures of Ar/$H_2O$. For the coating deposited at 800 mTorr, HA (0002) poles are randomly distributed over the sample directions 1, 2, and 3. The pole figures for the coating deposited at a pressure in the 700–600 mTorr display increased density of HA (0002) poles near the sample direction 3 ($\Psi = 0°$), indicating the *c*-axis texturing along the direction perpendicular to the coating surface. The pole figures for the coating deposited at 500 mTorr show again random orientation of HA crystallites with respect to any of the sample directions. Therefore, the texturing of HA can only be obtained at conditions that ensure not only high kinetic energy of plume species and efficient momentum transfer along the direction normal to the substrate, but also the sufficient supply of OH.

Initial cell attachment to the HA coatings with random and preferential crystallographic orientation was investigated by fluorescent microscopy. Briefly, cells were allowed to adhere to the surfaces for 1 h, and then cells were visualized by staining the actin cytoskeleton with phalloidin. Adherent cells on 3 distinct microscopic fields for each substrate were counted in order to obtain a quantitative measure of cell attachment. As shown in Figure 4, cells attached in greater numbers to the HA coatings with preferential *c*-axis texture, as compared with randomly-oriented coatings. Further studies are needed to elucidate the underlying mechanism regulating this effect.

## CONCLUSIONS

In summary, we have studied the crystallographic orientation of calcium phosphate polycrystalline coatings deposited by PLD and its effect on the behavior of human mesenchymal stem cells. High laser energy density and normal incidence of the laser plume lead to HA coatings whose grains have the *c*-axis preferentially aligned perpendicularly to the substrate. The preferred orientation of HA can only be obtained under conditions that ensure not only high kinetic energy of plume species and efficient momentum transfer along the direction normal to the substrate, but also sufficient supply of OH. Textured HA coatings seem to enable better cell attachment than randomly-oriented HA coatings. These findings may be relevant in the fabrication of textured HA coatings with improved mechanical properties and tailored bioactivity for biomedical applications and control of cell activity.

## ACKNOWLEDGMENTS

This research was supported by the National Institute of Dental and Craniofacial Research (NIDCR) under Grants R01 DE013952-04 and R01 AR51539. The coating fabrication was supported in part by a Major Research Instrumentation award from the National Science Foundation (NSF) under Grant No. DMR-0116098. The X-ray pole figure measurements at Carnegie Mellon University were supported by the Materials Research Science and Engineering Centers (MRSEC) program of the NSF under Award No. DMR-0520425.

## REFERENCES

1. U. F. Kocks, C. N. Tomé, and H.-R. Wenk, *Texture and anisotropy* (Cambridge University Press, 1998).
2. W. Tong, J. Chen, X. Li, J. Feng, Y. Cao, Z. Yang, and X. Zhang, *J. Mater. Sci.* **31**, 3739 (1996).
3. F. J. García-Sanz, M. B. Mayor, J. L. Arias, J. Pou, B. León, and M. Pérez-Amor, *J. Mater. Sci.-Mater. Med.* **8** (12), 861 (1997).
4. C. M. Roome and C. D. Adam, *Biomaterials* **16** (9), 691 (1995).
5. K. van Dijk, H. G. Schaeken, J. C. G. Wolke, C. H. M. Maree, F. H. P. M. Habraken, J. Verhoeven, and J. A. Jansen, *J. Biomed. Mater. Res.* **29**, 269 (1995).
6. L. L. Hench and J. Wilson, *An introduction to bioceramics* (World Scientific, 1993).
7. H. Kim, Y. K. Vohra, W. R. Lacefield, and R. P. Camata, *Mater. Res. Soc. Sym. Proc*. **750**, 71 (2003).
8. H. Kim, Y. K. Vohra, P. J. Louis, W. R. Lacefield, J. E. Lemons, and R. P. Camata, *Key Eng. Mater.* **284-286**, 207 (2005).
9. H. Kim, Y. K. Vohra, W. R. Lacefield, and R. P. Camata, *J. Mater. Sci.-Mater. Med.* **16** (10), 961 (2005).
10. J. S. Kallend, U. F. Kocks, A. D. Rollett, and H.-R. Wenk, *Mater. Sci. Eng. A* **132**, 1 (1991).
11. A. A. Sawyer, K. M. Hennessy, and S. L. Bellis, *Biomaterials* **26**, 1467 (2005).
12. N. Velisavljevic, Y. K. Vohra, *Appl. Phys. Lett.* **82**, 4271 (2003).